

High Field behavior of the Spin Gap compound $\text{Sr}_2\text{Cu}(\text{BO}_3)_2$

Suchitra E. Sebastian¹, D. Yin¹, P. Tanedo¹, G. A. Jorge¹, N. Harrison², M.

Jaime², Y. Mozharivskyj³, G. Miller³, J. Krzystek⁴, S. A. Zvyagin⁴, I. R. Fisher¹

¹*Geballe Laboratory for Advanced Materials and Department of Applied Physics, Stanford University, Stanford, CA 94305*

²*MST-NHMFLL, Los Alamos National Laboratory, Los Alamos, NM 87545*

³*Department of Chemistry, Iowa State University, Ames, IA 50011 and*

⁴*National High Magnetic Field Laboratory, Tallahassee, FL 32310*

(Dated: 8th February 2020)

We report magnetization and heat capacity measurements of single crystal samples of the spin gap compound $\text{Sr}_2\text{Cu}(\text{BO}_3)_2$. The material has a singlet ground state and low field data can be fit by an isolated dimer model with spin gap $\Delta=100\text{K}$. However, for fields that are large compared to the spin gap, triplet excitations are observed for significantly smaller fields than predicted by the isolated dimer model, indicating triplet delocalization due to inter-dimer coupling. Magnetization behavior at low temperatures suggests additional cooperative effects.

Recently, the spin gap system $\text{SrCu}_2(\text{BO}_3)_2$ which is a physical realization of the Shastry-Sutherland model [1], has received a considerable amount of interest [2-5]. Spin frustration in a network of connected dimers leads to competition between Neel and singlet dimer ground states, reducing the spin gap to $\sim 30\text{K}$. The relatively small spin gap enables the excited state magnetization to be probed - it has been found to be a series of fractional magnetic plateaus of the total magnetization, associated with localized triplet excitations in structures commensurate with the lattice. In this letter, we report results of our study of the first single crystals of the spin gap system $\text{Sr}_2\text{Cu}(\text{BO}_3)_2$ which although similar in composition to $\text{SrCu}_2(\text{BO}_3)_2$, has a very different magnetic lattice and exhibits novel magnetic properties associated with triplet delocalization.

$\text{Sr}_2\text{Cu}(\text{BO}_3)_2$ exists in two structural phases: here we describe the first measurements of single crystal samples of the high temperature $\beta\text{-Sr}_2\text{Cu}(\text{BO}_3)_2$ phase. This phase is thermodynamically stable above $\sim 800^\circ\text{C}$, so samples were quenched from 860°C to room temperature during the growth process. $\beta\text{-Sr}_2\text{Cu}(\text{BO}_3)_2$ has an orthorhombic unit cell with lattice parameters $a=7.612\text{\AA}$, $b=10.854\text{\AA}$ and $c=13.503\text{\AA}$ [6]. The structure is two-dimensional, comprising layers of $\text{Cu}_2\text{B}_4\text{O}_{12}$ containing Cu^{2+} ($3d^9$, $s=1/2$) ions, shown in Figure 1, separated by Sr ions [6]. Each layer comprises distorted octahedral $\text{Cu}(1)\text{O}_6$ units, square planar $\text{Cu}(2)\text{O}_4$ units and triangular $\text{B}(1,2,3)\text{O}_3$ units.

The Cu^{2+} ions are coupled via three different exchange pathways (shown as J, J' and J'' in Figure 2) via triangular BO_3 units. However, orthorhombic distortion of the $\text{Cu}(1)\text{O}_6$ octahedra lifts the e_g degeneracy (apical oxygen atoms are further from the central $\text{Cu}(1)$ atom at 2.49\AA and 2.42\AA , than the equatorial oxygen atoms, at 1.99\AA and 1.92\AA [6,7]), such that the highest energy level is the antibonding combination of $\text{Cu } 3d_{x^2-y^2}$ and the equatorial $\text{O } 2p_\sigma$ orbitals, and the $\text{Cu}(1) 3d^9$ hole must reside in the equatorial plane. The dominant exchange pathway is therefore J, through the equatorial oxygen

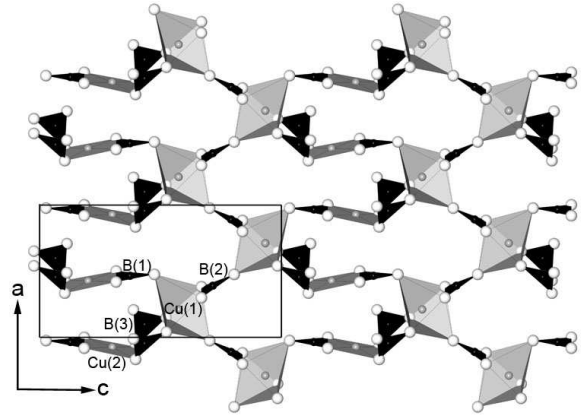


Figure 1: $\text{Cu}_2\text{B}_4\text{O}_{12}$ layers from $\beta\text{-Sr}_2\text{Cu}(\text{BO}_3)_2$. The open circles represent O, the gray circles Cu and the black circles B. Dimer units comprise $\text{Cu}(1)$ and $\text{Cu}(2)$ atoms linked via $\text{B}(3)\text{O}_3$ groups. Sr ions separating the layers are not shown.

ions of the $\text{Cu}(1)\text{O}_6$ octahedra. Hence, the equivalent magnetic lattice (shown in Figure 2) comprises essentially isolated dimer units with large intra-dimer exchange J between $\text{Cu}(1)$ and $\text{Cu}(2)$ through the $\text{B}(3)\text{O}_3$ triangular units.

Single crystals of $\beta\text{-Sr}_2\text{Cu}(\text{BO}_3)_2$ were grown using LiBO_2 as a flux [6]. The polycrystalline precursor was prepared by a solid state reaction of SrCO_3 , CuO and B_2O_3 ground together in stoichiometric ratios and heated in flowing O_2 at 900°C for approximately 72 hours with intermediate grindings. A mixture with 1:1.4 molar ratio of polycrystalline $\text{Sr}_2\text{Cu}(\text{BO}_3)_2$ to LiBO_2 was heated in a Pt crucible to 925°C , cooled at approximately 1°C per hr to 860°C and the remaining liquid decanted. The crystals were allowed to cool rapidly in air. The resulting single crystals of $\beta\text{-Sr}_2\text{Cu}(\text{BO}_3)_2$ were multi-faceted, purple in color, and had dimensions of up to 5mm on a side.

Magnetization measurements in fields up to 5 T were performed using a Quantum Design SQUID magnetome-

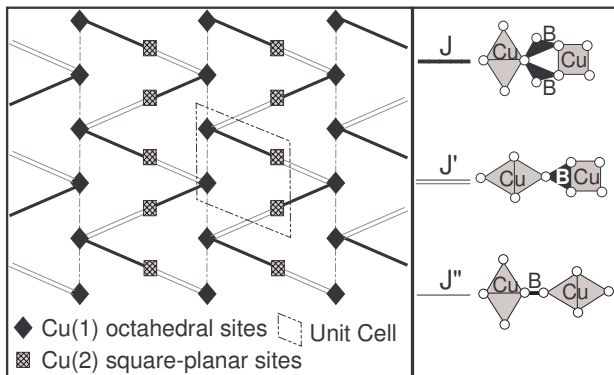


Figure 2: Equivalent magnetic lattice representing the structure of $\text{Cu}_2\text{B}_4\text{O}_{12}$ planes in $\text{SrCu}_2(\text{BO}_3)_2$. To the right, the legend for exchange pathways represented in the equivalent magnetic lattice ($J \gg J', J''$)

ter. DC magnetic susceptibility ($\chi = M/H$) measured in 5000 Oe with H aligned along the principal crystal axes is shown in Figure 3. For all three orientations, the magnetic susceptibility per mole of Cu spins as a function of temperature can be well fit by the isolated dimer model, (shown by the solid line in Figure 3) with an additional Curie term to account for a small concentration of isolated impurity spins:

$$\chi = \frac{N(\mu_B g)^2}{k_B T (3 + \exp(\Delta/T))} + C/T + \chi_0$$

where N is Avogadro's number, Δ the spin gap, C the Curie constant due to non-interacting impurities and χ_0 a temperature-independent term. In the absence of any interdimer interaction, Δ is given by the intradimer coupling J , but may be renormalized to a lower value in the case of small interdimer exchange. The value of Δ for all three orientations is found from these fits to be $100 \pm 1.5\text{K}$ in agreement with previous polycrystalline data [7]. Values for g are found to be 2.0 ± 0.05 for H aligned along the b and c -axes, but 2.2 ± 0.05 for H aligned along the a -axis, consistent with the orientation of the CuO_4 units. C varies from 0.001 to 0.003 emuK/molOe , corresponding to 0.3% to 0.8% impurity concentration, assuming impurity spins with $g=2$, $s=1/2$. The T -independent term χ_0 is small and positive, likely due to a very small concentration of ferromagnetic impurities. Values vary slightly between samples and with orientation, and for the data shown in Figure 3 correspond to approximately $10^{-4} \mu_B$ per formula unit.

Values for g were independently obtained via Electron Spin Resonance (ESR) using a Bruker Elexsys E680X spectrometer at X-band frequency 9.38 GHz at room temperature. These measurements gave $g_a = 2.230$, $g_b = 2.060$ and $g_c = 2.130 \pm 0.004$ in good agreement with values obtained from susceptibility fits.

The Schottky anomaly from the 100K spin gap is too

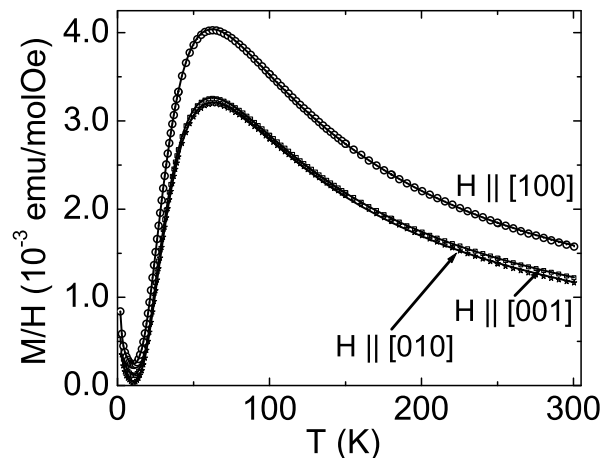


Figure 3: Temperature dependence of the magnetic susceptibility of a single crystal of $\text{Sr}_2\text{Cu}(\text{BO}_3)_2$ for a field of 5000 Oe aligned along the principal crystal axes. Solid lines show fit to isolated dimer model, described in main text.

small to be easily resolved against the large phonon contribution to the heat capacity. However, the shift in heat capacity due to Zeeman splitting of the triplet states in a magnetic field (reducing the spin gap) can be observed. Measurements were made in zero field and 18 T continuous field for a single crystal of $\beta\text{-Sr}_2\text{Cu}(\text{BO}_3)_2$ weighing 7.9 mg. The field was oriented at an arbitrary angle to the crystal. A calorimeter made of plastic materials and silicon was used, employing a thermal relaxation time technique. The difference between these two values, $\Delta C_p = C_p(18\text{T}) - C_p(0\text{T})$ is due solely to changes in the magnetic contribution and can be calculated for an isolated dimer model using average values for Δ and g . Figure 4 shows calculated and measured values for ΔC_p as a function of temperature. The measured data has a broad maximum with a peak value of $0.38 \pm 0.07 \text{ J/molK}$ centered at $14 \pm 1 \text{ K}$, compared to the model which has a peak value of 0.32 J/molK centered at 16 K. The good agreement between the data and the isolated dimer model confirms the description of the system as one of essentially isolated dimers (i.e. $J \gg J', J''$) in fields that are low compared to the spin gap.

We note that additional features are evident in the heat capacity at high temperatures (inset to figure 4), which appear to be unrelated to the low temperature magnetic properties. Structural refinements performed on a single crystal indicate no change in symmetry or average atomic positions between the Low Temperature (LT) ($T < 230 \text{ K}$), Room Temperature (RT) ($230 \text{ K} < T < 320 \text{ K}$), and High Temperature (HT) ($T > 320 \text{ K}$) regions, but a marked change in the thermal parameters of the B atoms indicates a change in vibrational properties.

The behavior of $\text{Sr}_2\text{Cu}(\text{BO}_3)_2$ is particularly interest-

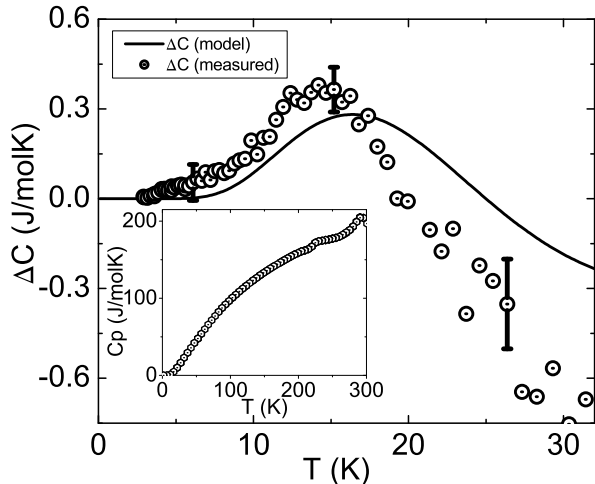


Figure 4: Difference in heat capacity $\Delta C_p = C_p(18 \text{ T}) - C_p(0 \text{ T})$ for a single crystal of $\text{Sr}_2\text{Cu}(\text{BO}_3)_2$. Solid line shows calculated value for dimer model with $\Delta = 100 \text{ K}$ and $g=2.14$. Inset shows total heat capacity in zero field between 2K and 300K. Mol refers to the formula unit.

ing in high magnetic fields, for which $g\mu_B H \sim k_B \Delta$. We find that the magnetization can no longer be fit to the isolated dimer model, indicating the effect of interdimer coupling. Magnetization measurements were made in pulsed high magnetic fields up to 65 T at different temperatures. The data are obtained using a wire-wound sample extraction magnetometer in which the sample is inserted or removed from the detection coils *in situ*. Data were taken for increasing and decreasing fields, and the average value calculated. A collection of six randomly oriented fragments from a clean single crystal was used in order to maximize the filling factor of the coil. Magnetization for this composite sample as a function of field is shown in Figure 5. A small linear diamagnetic contribution with negative slope $9 \times 10^{-4} \mu_B/\text{T}$, due to the response of the source coils, has been subtracted from the data. The value of magnetization at 50 K in a field of 5 T was compared with SQUID magnetometer magnetization data in order to obtain absolute values for the magnetization in units of μ_B/Cu .

A feature of the isolated dimer model is a sharp increase in magnetization to $1 \mu_B$ when the lowest Zeeman-split triplet state crosses the singlet state at $T = 0$. For $\Delta = 100 \text{ K}$ and $g=2.14$ (i.e. average value for the composite sample), this would occur at an applied magnetic field $H_c = 69 \text{ T}$ if there was no interdimer interaction, with thermal broadening at finite temperatures (solid lines in Figure 5). As shown in Figure 5, $M(H)$ data correspond very closely to this model for temperatures of 20 K and above, but deviate significantly for lower temperatures. At 1.5 K, data taken to 65 T clearly show the swift rise

in magnetization due to triplet excitations. This occurs at a magnetic field lower than the spin gap Δ . Furthermore, data for temperatures of 5 and 10 K coincide with the 1.5 K data within experimental uncertainty.

The deviation from the isolated dimer model is clearly revealed in a graph of magnetization as a function of temperature (Figure 6). In high magnetic fields, the magnetization does not fall to zero at low temperatures, and instead, is as large as $0.15 \mu_B$ for temperatures below 10 K. Above 15 K, the $M(T)$ curves rise sharply, coinciding with the isolated dimer model for temperatures above 20 K.

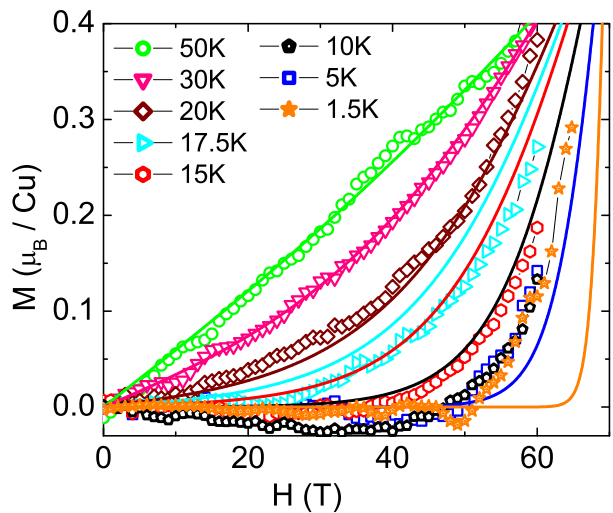


Figure 5: Magnetization of $\text{Sr}_2\text{Cu}(\text{BO}_3)_2$ as a function of applied field at different temperatures. Calculated values for isolated dimer model with $J = 100 \text{ K}$ and $g=2.14$ shown by solid lines.

The observed magnetization behavior indicates that at low temperatures, the isolated dimer model is not an accurate description of $\text{Sr}_2\text{Cu}(\text{BO}_3)_2$ in magnetic fields that are large compared to the spin gap. The upturn in magnetization due to the excitation of singlet to triplet states occurs at a lower magnetic field $H_c \sim 56 \text{ T}$ than predicted by the isolated dimer model (67 - 74 T, for g values between 2.2 and 2.0), indicating that the interdimer exchange terms J' and J'' have a significant effect. This effect can be estimated if we assume that J' and J'' are much smaller than J and therefore can be treated as a perturbation to the isolated dimer model. The interdimer terms (which do not have an effect on $S^z=0$ states) cause triplet delocalization by acting on $S^z=1$ triplet states, enabling triplet hopping from first order in the perturbation solution and resulting in a dispersion relation that reduces H_c from $k_B \Delta / g\mu_B$. This is very different from the Shastry Sutherland compound $\text{SrCu}_2(\text{BO}_3)_2$, for which triplets are localized up to the

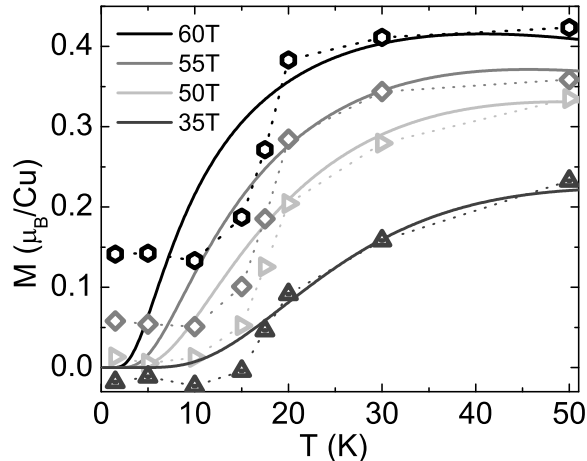


Figure 6: Magnetization as a function of temperature for different magnetic fields. Symbols (connected by dotted lines to guide the eye) indicate measured magnetization data extracted from Figure 5, solid lines indicate isolated dimer model with $J = 100$ K and $g=2.14$

fourth order in the perturbation solution, due to frustration [4]. To obtain an estimate of H_c in $\beta\text{-Sr}_2\text{Cu}(\text{BO}_3)_2$, the simplifying assumption can be made that in the vicinity of level crossing, the eigenspace comprises only the two degenerate singlet ($S=0$) and lowest triplet ($S^z=1$) states. The $\text{Cu}_2\text{B}_4\text{O}_{12}$ planes in $\beta\text{-Sr}_2\text{Cu}(\text{BO}_3)_2$ (Figure 2) can then be mapped on to a square lattice of hardcore bosons, in which the links represent J' and J'' , and each vertex is occupied by a boson (representing a triplet) or remains unoccupied (representing a singlet.) From the first order perturbation solution, the observed reduction in H_c from the spin gap $k_B\Delta/g\mu_B$ (corresponding to the shift in magnetization of 11-18 T depending on the value of g) is then given by $(J'+J'')/2$ [8]. For the lower limit of $k_B\Delta/g\mu_B - H_c \simeq 11\text{T}$, we obtain $(J'+J'')/2 \sim 17\text{K}$. Further experiments are in preparation to independently determine these values and to directly measure the triplet dispersion.

At low temperatures and in high magnetic fields, interactions between the triplets will determine the nature of the ground state. The temperature independent finite magnetization below 20K in high magnetic fields (Figure 6) is presumably associated with this state. For delocalized triplets, in the absence of anisotropic interactions in the Hamiltonian, one possibility for the ordered ground state is a Bose Einstein Condensate, similar to that observed in TlCuCl_3 [9,10]. It is intriguing to consider this

possibility, but it is also important to note that in this case only a small portion of the phase diagram is accessible due to the large value of the spin gap, and even at 60T the magnetization only reaches $0.15\mu_B$, corresponding to a small 15% concentration of triplets. This means that it will be difficult to unambiguously identify the nature of the ground state in high magnetic fields for this material.

In summary, we have made the first magnetization and heat capacity measurements of single crystals of the spin gap compound $\beta\text{-Sr}_2\text{Cu}(\text{BO}_3)_2$. In low magnetic fields, the material behaves similar to an isolated dimer system with a spin gap $\Delta = 100$ K, as observed from both magnetization and heat capacity measurements. However, in magnetic fields which are large compared to Δ , interdimer exchange interactions reduce H_c , the field required to produce triplet excitations. For fields above H_c , cooperative effects presumably lead to an ordered ground state, the nature of which remains to be determined. Further experiments on this and related materials will undoubtedly clarify our understanding of the role of weak interdimer coupling in determining the high field behavior of singlet compounds.

We gratefully acknowledge helpful discussions with C. Batista. This work is supported by the National Science Foundation, Division of Materials Research under DMR-0134613. Experiments performed at the National High Magnetic Field Laboratory were supported by the National Science Foundation through Cooperative Grant No. DMR-9016241 and MRI Grant No. 0079641, the State of Florida, and the Department of Energy. I.R.F acknowledges support from the Alfred P. Sloan Foundation. S.E.S acknowledges support from the Mustard Seed Foundation.

-
- [1] B. S. Shastry and B. Sutherland, *Physica* **108B**, 1069 (1981).
 - [2] R. W. Smith and D. A. Keszler, *J. Solid State Chem.* **93**, 430 (1991).
 - [3] H. Kageyama *et al.*, *Phys. Rev. Lett.* **82**, 3168 (1999).
 - [4] S. Miyahara and K. Ueda, *Phys. Rev. Lett.* **82**, 3701 (1999).
 - [5] H. Kageyama *et al.*, *J. Phys. Soc. Jpn.* **68**, 1821 (1999).
 - [6] R. W. Smith and D. A. Keszler, *J. Solid State Chem.* **81**, 305 (1989).
 - [7] H. Sakurai *et al.*, *J. Phys. Soc. Jpn.* **71**, 999 (2001).
 - [8] F. Mila, *Eur. Phys. J. B* **6**, 201 (1998).
 - [9] Ch. Rugg *et al.*, *Nature* **423**, 62 (2003).
 - [10] T. Nikuni *et al.*, *Phys. Rev. Lett.* **84**, 5868 (2000).